



Published in final edited form as:

Biochemistry. 2011 July 5; 50(26): 5813–5815. doi:10.1021/bi200794c.

Oxidation and Loss of Heme in Soluble Guanylyl Cyclase from *Manduca sexta*[†]

Bradley G. Fritz, Xiaohui Hu, Jacqueline L. Brailey, Robert E. Berry, F. Ann Walker, and William R. Montfort^{*}

Department of Chemistry and Biochemistry, University of Arizona, Tucson, Arizona, 85721

Abstract

Oxidation and loss of heme in soluble guanylyl/guanylate cyclase (sGC), the nitric oxide receptor, is thought to be a major contributor to cardiovascular disease and is the target of compounds BAY 58-2667 and HMR1766. Using spectroelectrochemical titration, we found a truncated sGC to be highly stable in the ferrous state (+234 mV) and to bind ferrous heme tightly even in the presence of NO, despite the NO-induced release of the proximal histidine. In contrast, oxidized sGC readily loses ferric heme to myoglobin ($0.47 \pm 0.02 \text{ hr}^{-1}$). Peroxynitrite, the presumed cellular oxidant, readily oxidizes sGC in 5 mM glutathione.

The biological production of nitric oxide (NO), a free-radical molecule, is vital to the development and function of nearly all animals. NO is produced by NO synthase and regulates numerous physiological activities, including blood pressure, wound healing and memory formation. The NO signal is propagated through the heme-containing enzyme soluble guanylyl cyclase (sGC), an ~150 kDa heterodimeric protein that may reside in the same cell as NO synthase, or in nearby cells. The two sGC subunits are gene duplications with each containing H-NOX, PAS, coiled-coil and cyclase domains (1). NO binds to ferrous heme in the β subunit, which leads to rupture of the proximal histidine bond, stimulation of cyclase activity and the conversion of GTP to cGMP. A variety of tissue-specific physiological responses can result, including smooth muscle relaxation and vasodilation. There are no structures of sGC, but several structures of bacterial H-NOX proteins have been determined and reveal a single-domain fold with a deep hydrophobic cleft for heme binding (2–4).

sGC is prone to heme loss during isolation (5) and apparently also in the cell, particularly after oxidation, which can occur, for example, during inflammation or heart failure. Compounds BAY 58-2667 (cinaciguat) and HMR1766 (ataciguat) were designed to rescue apo-sGC by filling the heme pocket, leading to an sGC complex with high catalytic activity and decreased turnover in the cell (6–11). Investigations into the stability of the sGC heme, its reduction potential and its propensity for loss are needed but have been challenging to pursue, due in part to the difficulty in working with the protein.

[†]Funding sources: This work was supported by National Institutes of Health grants HL062969 and GM077390 (WRM), HL054826 (FAW) and T32 GM008804 (BGF), and by American Heart Association grants 10PRE2630177 (BGF) and 0515517Z (XH).

^{*}Corresponding author: William R. Montfort, Dept. of Chemistry and Biochemistry, University of Arizona, Tucson, Arizona, 85721; Tel:(520) 621-1884; Fax: (520) 626-9204; montfort@email.arizona.edu.

ASSOCIATED CONTENT

Supporting Information. Materials and Methods and Tables S1-S5. This material is available free of charge via the Internet at <http://pubs.acs.org>.

We have produced several recombinant forms of sGC from *Manduca sexta*, the tobacco hornworm, that include H-NOX, PAS and coiled-coil domains of both α and β subunits, but not the cyclase domains, and display greater stability than does the full-length protein (12, 13) (Supplementary Fig. S1). These proteins are bacterially expressed with an intact ferrous heme, display CO and NO binding that is similar to that for the full-length protein, and respond to allosteric stimulators 3-(5'-hydroxymethyl-2'-furyl)-1-benzylindazole (YC-1) and BAY 41-2272 (12, 13). Here, we make use of previously described construct *Ms* sGC-NT1 (α 1-471, β 1-401) to measure the heme reduction potential, and newly developed *Ms* sGC-NT13 (α 49-450, β 1-380) to measure heme loss kinetics. Construct *Ms* sGC-NT13 was trimmed to remove the first 48 residues from the α subunit, which are predicted to be disordered, and 21 residues from the C-termini of both α and β subunits, which are predicted to link the coiled-coil and cyclase domains, leading to a protein with increased levels of expression and stability. Ferrous, unliganded *Ms* sGC-NT13, as well as its complexes with CO and YC-1, is stable at room temperature on the time-scale of days to weeks with no change in Soret absorbance maxima position or intensity. The Soret absorbance maxima for unliganded *Ms* sGC-NT13 (433 nm), its complexes with CO (423 nm), CO/YC-1 (422 nm) and NO (400 nm), and after oxidation (394 nm), correspond with values previously published for *Ms* sGC (12) and other mammalian sGC proteins (14).

One of the remarkable properties of heme as a protein cofactor is the degree to which heme reduction potential and ligand specificity can be tuned by the protein for the job at hand. We determined the midpoint potential for *Ms* sGC-NT1 by spectroelectrochemical titration at three pH values (Fig. 1, Table 1). *Ms* sGC has an unusually high midpoint potential for a *b*-type heme, +234 mV at pH 7.4, which stabilizes the ferrous state. This value is relatively insensitive to small changes in pH, indicating the absence of ionizable groups near the heme, including heme-ligated water, that have pK_a values below 10. Binding of compound YC-1, which allosterically stimulates sGC and blocks escape of both CO and NO from the *Ms* sGC-NT2 heme pocket (12, 13), leads to a small (22 mV) increase in measured reduction potential (Fig. 1, Table 1), consistent with an increase in heme pocket desolvation upon YC-1 binding.

Although NO binds to both ferri- and ferroheme centers, ferroheme provides at least two functional advantages for sGC. First, binding of NO to ferrous heme is extremely tight, exhibiting dissociation constants in the picomolar to femtomolar range. This allows for very low NO concentrations to initiate the signaling cascade and for avoiding the higher NO concentrations that give rise to nitrosative stress. Recent estimates for typical NO concentrations of importance for signaling *in vivo* are between 0.1 and 5 nM (15). Second, the *trans* effect of NO binding is particularly prominent for ferroheme (16), allowing for proximal histidine release and the propagation of an NO-dependent conformational change from the heme pocket to the catalytic center.

The measured reduction potential of *Ms* sGC-NT1 is approximately 200 mV more positive than that of myoglobin (17), and 67 mV more positive than that of the oxygen-binding *Tt* H-NOX protein (18), both of which function as ferroheme proteins. The ferriheme nitrophorins from *Rhodnius prolixus*, which transport NO from the insect saliva to a victim during blood feeding, maintain a midpoint potential of approximately -300 mV (19), over half a volt more negative than that of sGC. The ferriheme allows the nitrophorins to readily bind, transport and release NO. How heme-proteins acquire an appropriate midpoint potential is incompletely understood but likely involves electrostatic stabilization, influence of coordinating ligands, and heme geometry. The *Rhodnius* nitrophorins achieve their negative reduction potential in part through judicious placement of negatively charged side chains inside the protein, which stabilizes the positively charged ferric heme (20), and through heme ruffling distortion, which mixes porphyrin and metal orbitals to stabilize Fe(III) and

disfavor heme reduction (21, 22). Myoglobin has a partially polar heme pocket and a relatively planar heme, even when bound to NO (23). The H-NOX proteins, however, have very hydrophobic heme pockets (2–4), which favor neutral ferrous heme, but are also highly distorted, which should disfavor ferrous heme, but may not, based on results from site-directed mutagenesis of *Tt* H-NOX (18, 24). In those experiments, mutations leading to decreased heme distortion also lead to decreased reduction potentials at the pH examined. However, the mutations alter the pK_a of the water ligand axial to the ferric heme (24), suggesting the reduction potential may have substantial pH dependence. A homology model of the *Ms* sGC β H-NOX domain (12) suggests that sGC has an even more hydrophobic pocket than *Tt* H-NOX (Fig. S2), which is consistent with the more positive midpoint potential presented here and its invariance with pH (Table 1).

To assess rates of heme loss in *Ms* sGC, we adapted the approach of Hargrove *et al.* using a H64Y/V68F myoglobin variant that has a distinct absorbance spectra and a unique green color (25). Addition of hemin to the apo protein led to a ferric (met) myoglobin with Soret and α/β band absorbance maxima of 411 and 600 nm, respectively (Fig. S3A). Excess YC-1 had no effect on hemin uptake by the apo-myoglobin (ApoMb). Addition of ferrous hemin led to a ferrous myoglobin with Soret and α/β band absorbance maxima of 428 and 560 nm respectively.

We investigated the transfer of heme from *Ms* sGC-NT13 to 10-fold excess ApoMb under a variety of conditions. No loss of heme was detected from ferrous *Ms* sGC, its CO complex or its CO/YC-1 complex over a 15 hr period (Fig. S3), suggesting that ferrous heme either does not escape from *Ms* sGC in this time period, or binding is substantially tighter to ferrous *Ms* sGC than to ApoMb. Interestingly, the ferrous sGC-NO complex, which is five-coordinate after cleavage of the proximal histidine bond, retains high heme affinity and does not lose heme to ApoMb (Fig. 2A). Under anaerobic conditions, the sGC-NO complex is completely stable in both the presence and absence of ApoMb, but will slowly lose NO under aerobic conditions, presumably through NO release and reaction with dioxygen (Fig. S4). Addition of YC-1, which slows NO release, completely stabilizes the sGC-NO complex over 15 hr.

In contrast, oxidation of *Ms* sGC-NT13 and addition of ApoMb leads to loss of absorbance at 396 nm and gain of absorbance at 411 nm (Fig. 2B), indicating heme transfer from *Ms* sGC to ApoMb. Transfer is relatively rapid at 20°C and occurs with a first order rate constant of $0.55 \pm 0.02 \text{ hr}^{-1}$ (Fig. 2C), which is 20 to 80 times faster than loss of heme from native sperm whale metmyoglobin at 37°C, depending on pH conditions (0.007 hr^{-1} at pH 7.0, and 0.03 hr^{-1} at pH 8.0, (25)). A strong increase in absorbance at 280 nm in addition to a large drift in the baseline signal over the course of the experiment, results from precipitation of apo-*Ms* sGC. In the presence of YC-1, the rate of ferriheme loss and the propensity toward precipitation are unchanged (Fig 2C).

Peroxynitrite (ONOO^-) formation from the reaction of NO and superoxide (O_2^-) is thought to occur *in vivo* during inflammation and to directly oxidize sGC heme (8, 26). To investigate this possibility, we added $\sim 80 \mu\text{M}$ peroxynitrite to $5 \mu\text{M}$ *Ms* sGC-NT13 while monitoring the sGC spectra. Conversion of the ferrous heme to ferric was rapid and complete (Fig. S5A), and completely reversible with sodium dithionite, a strong reductant. Addition of 5 mM reduced glutathione, the major reductant in the cytosol and present at 1–10 mM, was only able to partially re-reduce oxidized sGC. Addition of $\sim 160 \mu\text{M}$ peroxynitrite to $5 \mu\text{M}$ sGC in a buffer containing 5 mM GSH still yielded a small percentage of oxidized sGC, which remained unchanged after 1 hr (Fig. S5B). Taken together, these data suggest that peroxynitrite can lead to oxidized sGC under cellular conditions, supporting proposals of this mechanism for sGC oxidation *in vivo*.

In summary, *Ms* sGC is highly stabilized toward the ferrous state ($E^\circ = +234$ mV) and, when ferrous, is highly resistant to heme loss both in the absence and presence of NO. Heme oxidation leads to a highly unstable protein that readily loses heme ($t_{1/2} = 76$ min). Peroxynitrite rapidly oxidizes the ferrous heme and can occur even in the presence of 5 mM glutathione. These data are consistent with the proposed mechanism for compounds BAY 58-2667 and HMR1766 in overcoming loss of sGC activity during oxidative stress in the cell, which is thought to occur by filling the apo-sGC heme pocket and rescuing the protein, leading to an activated and stabilized sGC molecule (6, 8, 9). Our data also highlight the stability of the ferrous heme complex even in the absence of a proximal histidine bond, as occurs in the Fe(II)-NO complex. Loss of Fe(III) heme in sGC appears to be driven by the unfavorable energetics of burying the positively charged heme center (formally +1) in a highly non-polar heme pocket.

Supplementary Material

Refer to Web version on PubMed Central for supplementary material.

Acknowledgments

We are grateful to Dr. Katrina Miranda for providing DEA/NO, Dr. John Olson for providing the myoglobin expression plasmid, and Dr. Sue Roberts for homology modeling.

References

1. Poulos TL. *Curr Opin Struct Biol.* 2006; 16:736–743. [PubMed: 17015012]
2. Nioche P, Berka V, Vipond J, Minton N, Tsai AL, Raman CS. *Science.* 2004; 306:1550–1553. [PubMed: 15472039]
3. Pellicena P, Karow DS, Boon EM, Marletta MA, Kuriyan J. *Proc Natl Acad Sci USA.* 2004; 101:12854–12859. [PubMed: 15326296]
4. Ma X, Sayed N, Beuve A, van den Akker F. *EMBO J.* 2007; 26:578–588. [PubMed: 17215864]
5. Ohlstein EH, Wood KS, Ignarro LJ. *Arch Biochem Biophys.* 1982; 218:187–198. [PubMed: 6128958]
6. Schmidt PM, Schramm M, Schroder H, Wunder F, Stasch JP. *J Biol Chem.* 2004; 279:3025–3032. [PubMed: 14570894]
7. Meurer S, Pioch S, Pabst T, Opitz N, Schmidt PM, Beckhaus T, Wagner K, Matt S, Gegenbauer K, Geschka S, Karas M, Stasch JP, Schmidt HH, Muller-Esterl W. *Circ Res.* 2009; 105:33–41. [PubMed: 19478201]
8. Hoffmann LS, Schmidt PM, Keim Y, Schaefer S, Schmidt HH, Stasch JP. *Br J Pharmacol.* 2009; 157:781–795. [PubMed: 19466990]
9. Martin F, Baskaran P, Ma X, Dunten PW, Schaefer M, Stasch JP, Beuve A, van den Akker F. *J Biol Chem.* 2010; 285:22651–22657. [PubMed: 20463019]
10. Schindler U, Strobel H, Schonafinger K, Linz W, Lohn M, Martorana PA, Rutten H, Schindler PW, Busch AE, Sohn M, Topfer A, Pistorius A, Jannek C, Mulsch A. *Mol Pharmacol.* 2006; 69:1260–1268. [PubMed: 16332991]
11. Zhou Z, Pyriochou A, Kotanidou A, Dalkas G, van Eickels M, Spyroulias G, Roussos C, Papapetropoulos A. *Am J Physiol Heart Circ Physiol.* 2008; 295:H1763–1771. [PubMed: 18757489]
12. Hu X, Murata LB, Weichsel A, Brailey JL, Roberts SA, Nighorn A, Montfort WR. *J Biol Chem.* 2008; 283:20968–20977. [PubMed: 18515359]
13. Hu X, Feng C, Hazzard JT, Tollin G, Montfort WR. *J Am Chem Soc.* 2008; 130:15748–15749. [PubMed: 18980304]
14. Karow DS, Pan D, Davis JH, Behrends S, Mathies RA, Marletta MA. *Biochemistry.* 2005; 44:16266–16274. [PubMed: 16331987]

15. Hall CN, Garthwaite J. Nitric Oxide. 2009; 21:92–103. [PubMed: 19602444]
16. Wyllie GR, Scheidt WR. Chem Rev. 2002; 102:1067–1090. [PubMed: 11942787]
17. Ding XD, Weichsel A, Andersen JF, Shokhireva TK, Balfour C, Pierik AJ, Averill BA, Montfort WR, Walker FA. J Am Chem Soc. 1999; 121:128–138.
18. Olea C, Boon EM, Pellicena P, Kuriyan J, Marletta MA. ACS Chem Biol. 2008; 3:703–710. [PubMed: 19032091]
19. Andersen JF, Ding XD, Balfour C, Shokhireva TK, Champagne DE, Walker FA, Montfort WR. Biochemistry. 2000; 39:10118–10131. [PubMed: 10956000]
20. Berry RE, Shokhirev MN, Ho AY, Yang F, Shokhireva TK, Zhang H, Weichsel A, Montfort WR, Walker FA. J Am Chem Soc. 2009; 131:2313–2327. [PubMed: 19175316]
21. Shokhireva T, Berry RE, Uno E, Balfour CA, Zhang H, Walker FA. Proc Natl Acad Sci USA. 2003; 100:3778–3783. [PubMed: 12642672]
22. Maes EM, Roberts SA, Weichsel A, Montfort WR. Biochemistry. 2005; 44:12690–12699. [PubMed: 16171383]
23. Schreiter ER, Rodriguez MM, Weichsel A, Montfort WR, Bonaventura J. J Biol Chem. 2007; 282:19773–19780. [PubMed: 17488722]
24. Olea C Jr, Kuriyan J, Marletta MA. J Am Chem Soc. 132:12794–12795. [PubMed: 20735135]
25. Hargrove MS, Singleton EW, Quillin ML, Ortiz LA, Phillips GN Jr, Olson JS, Mathews AJ. J Biol Chem. 1994; 269:4207–4214. [PubMed: 8307983]
26. Kagota S, Tada Y, Nejime N, Nakamura K, Kunitomo M, Shinozuka K. J Pharmacol Sci. 2009; 109:556–564. [PubMed: 19346675]

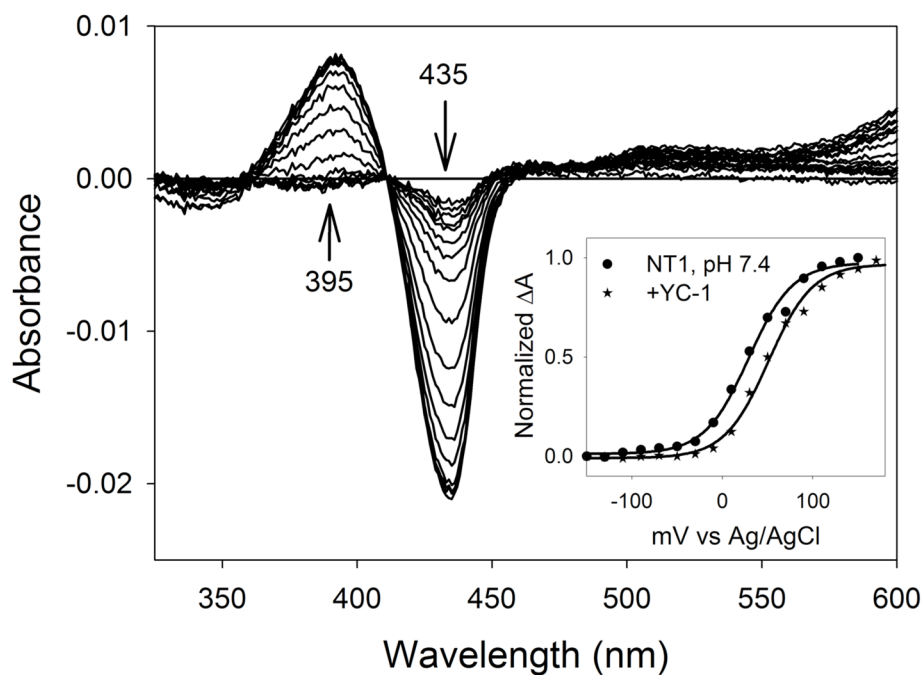
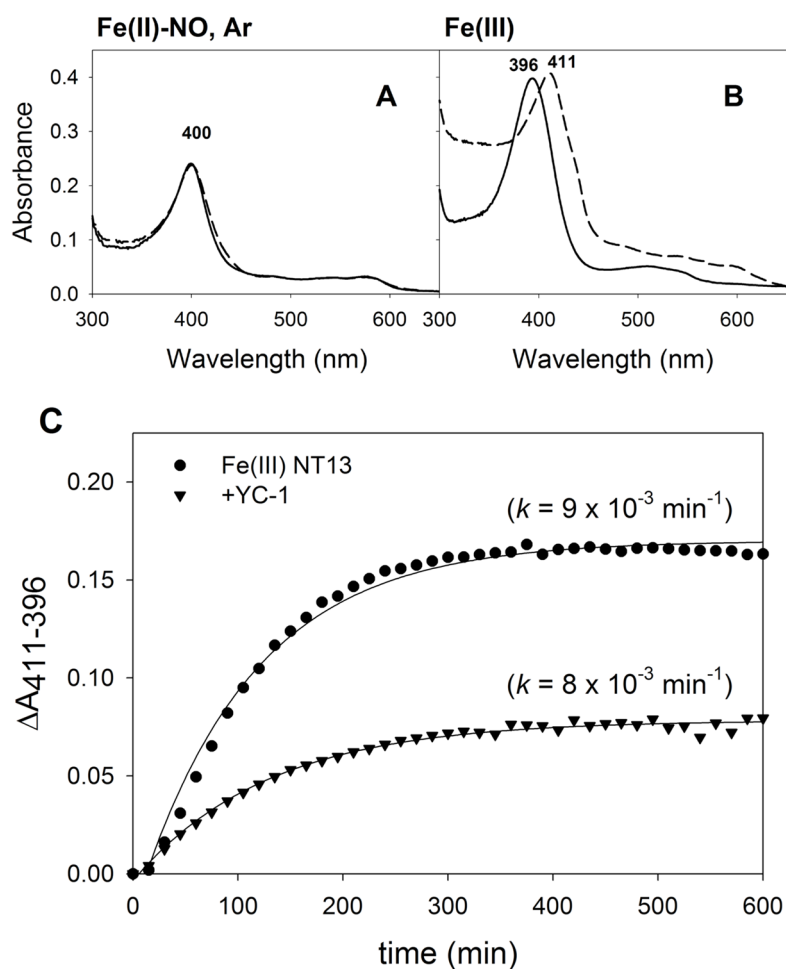


FIGURE 1. Spectroelectrochemical titration of *Ms* sGC-NT1. Applied voltages were from -150 to $+170$ mV vs. Ag/AgCl in 20 mV increments (add 205 mV for potential vs. NHE). Inset: Nernst plots \pm YC-1. YC-1 shifts the Nernst plot right, indicating an increased reduction potential of *Ms* sGC-NT1. Measurements were carried out in protein buffer containing 50 mM potassium phosphate, pH 7.4, 100 mM KCl and 5% glycerol

**FIGURE 2.**

Heme loss measurements. All samples contained $2 \mu\text{M}$ *Ms* sGC-NT13 and $20 \mu\text{M}$ ApoMb H64Y/V68F. **A.** *Ms* sGC-NT13 NO-complex (ferrous) formed with 10-fold excess of DEA/NO at 0 (solid line) and 15 hr (dashed line) under saturating Argon. No change in the heme Soret band is observed, indicating no loss of heme to ApoMb. **B.** Ferric *Ms* sGC-NT13 (solid line) loses heme to ApoMb, forming metmyoglobin (dashed line). **C.** Absorbance change ($\Delta A_{411-396}$) plotted versus time for the loss of *Ms* sGC (Soret maximum 396 nm) and subsequent formation of metmyoglobin (Soret maximum 411 nm), \pm YC-1. Rates were determined by a fit to a 3-parameter single exponential using SigmaPlot.

Table 1*Ms* sGC-NT1 midpoint potentials (mV)

pH	7.0	7.4	8.0
-	241 ± 2	234 ± 3	228 ± 2
+ YC-1 ^a	ND ^b	256 ± 2	ND ^b

^a 50 μM.^b Not determined.